*J. Fluid Mech.* (1979), *vol.* 90, *part* 3, *pp.* 531–539
*Printed in Great Britain*



# Flow structure of the free round turbulent jet in the initial region

By L. BOGUSŁAWSKI AND CZ. O. POPIEL

Heat and Mass Transfer Laboratory, Technical
University of Poznań, Poland

(Received 3 January 1978)

This note presents measurements of radial and axial distributions of mean velocity, turbulent intensities and kinetic energy as well as radial distributions of the turbulent shear stress in the initial region of a turbulent air jet issuing from a long round pipe into still air. The pipe flow is transformed relatively smoothly into a jet flow. In the core subregion the mean centre-line velocity decreases slightly. The highest turbulence occurs at an axial distance of about $6d$ and radius of (0·7 to 0·8)$d$. On the axis the highest turbulent kinetic energy appears at a distance of (7·5 to 8·5)$d$. Normalized distributions of the turbulent quantities are in good agreement with known data on the developed region of jets issuing from short nozzles.

## 1. Introduction

The axisymmetric turbulent free jet has been described in several monographs: Abramovich (1963), Ginievski (1969), Abramovich *et al.* (1974), Hinze (1975) and Rajaratnam (1976). Most of the published results describe the region far downstream of the nozzle where the flow structure is self-preserving. There are few experimental data concerning the developing region. Crow & Champagne (1971) examined the organized structure in the initial region of a round turbulent jet. Above a Reynolds number of $10^3$ the round jet may be treated as turbulent, however outside the core subregion there is an oscillatory mode of flow (up to about 10 diameters). The conical core of the jet within the first 4 diameters is surrounded by a wedge-shaped mixing subregion, including short interfacial waves. Beyond the core a tenuous train of large-scale vortex puffs appears with an average Strouhal number of about 0·30 based on the frequency, nozzle diameter and exit velocity. Lau & Fisher (1975) suggest that the mixing subregion contains an axial array of possibly toroidal vortices convecting downstream at about 0·65 times the nozzle efflux velocity. Sami, Carmody & Rouse (1967) investigated experimentally the turbulent structure in the developing region of an air jet issuing from a short nozzle with a Reynolds number of $22 \times 10^4$. Their measurements of turbulent shear stress are very doubtful. Also, Hill (1972) measured the local entrainment rate in the initial region of a jet using the porous-wall technique.

The flow structure in the developing region of the jet is important in many applications; for instance, impinging jets are used for the augmentation of convective heat or mass transfer processes. This note reports the results of measurements of flow structure in the initial region of a turbulent air jet issuing from a long circular pipe (with a fully developed turbulent velocity profile at the outlet section). This sort of

exit condition (as well as that of a short nozzle, which gives a rectangular velocity profile) occurs frequently in practice. Moreover, the free jet produced by a long circular pipe can be used in laboratories as a very easily reproduced model of known turbulent flows.

## 2. Experimental equipment

Figure 1 shows schematically the main parts of the instrumentation employed in the investigation. The isothermal axisymmetric turbulent air jet emerged from a circular pipe 38·5 mm in diameter and 50 diameters in length into still air of the same temperature. The constancy of the jet volume flow rate and temperature was checked by a Pitot tube and copper–constantan thermocouple at the inlet section of the pipe. A straightening honeycomb and an equalizing nozzle were situated upstream of the jet pipe.

The mean velocity, root-mean-square turbulent velocity fluctuations and the turbulent shear stress were measured with a two-channel constant-temperature thermo-anemometer (Thermo-Systems Inc.). The two measured values could be recorded simultaneously with a two-pen $X-Y_1$, $Y_2$ recorder using a single or X-probe. The displacement of the sensor was transformed to a voltage signal using a two-photodiode transducer and an impulse-digit-voltage sweep drive unit (Popiel, Kamasa & Bogusławski 1976) and was then transmitted to the recorder as the $X$ co-ordinate. The sensor position was observed with a collimator whose optical axis was parallel to the jet axis. Hot-wire sensors of diameter 3·8 $\mu$m with a frequency below 40 kHz were employed. The accuracy of polynomial linearization of the voltage signal and the accuracy of calibration were better than 2 %.

## 3. Results

The evolution of the longitudinal mean velocity profile is shown in figure 2. At the efflux section, the flow has the characteristic features of fully developed turbulent pipe flow. At distances beyond $8d$ the velocity profile becomes self-similar and is well approximated by

$$U/U_0 = \exp\{-108[r/(x+a)]^2\} \tag{1}$$

while the centre-line velocity decays roughly as (see figures 3 and 6)

$$U_0/U_{00} = Ad/(x+a), \tag{2}$$

where $A = 5{\cdot}9$ is a constant and $a = -0{\cdot}5d$ is the distance of the virtual source of the jet from the efflux section. Both expressions are recommended by Hinze (1975) and based on measurements obtained by Hinze & Van der Hegge Zijnen (1949) for a jet with a rectangular initial velocity profile. The rate of velocity spread deduced from (1) is $r_{0{\cdot}5}/(x+a) = 0{\cdot}080$, where $r_{0{\cdot}5}$ denotes the radius at which the velocity is half its maximum value. For the fully developed jet Rodi (1975) gives the rate $r_{0{\cdot}5}/x = 0{\cdot}086$ while the measurements of Donaldson, Snedeker & Margolis (1971) yield the value $r_{0{\cdot}5}/x = 0{\cdot}093$. The entrainment rates obtained by integration of the measured velocity profiles, presented in figure 4, can be described by the linear relation

$$m_E/m_{00} = 0{\cdot}183\,x/d \tag{3}$$

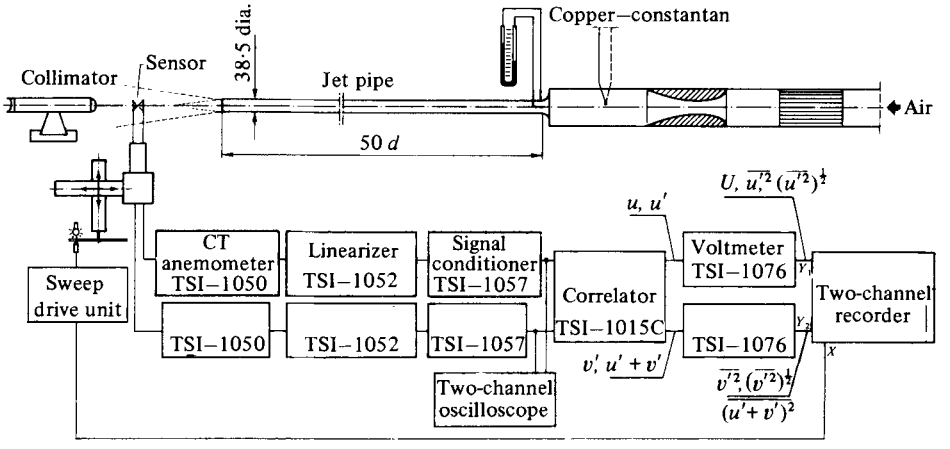


FIGURE 1. Experimental apparatus.

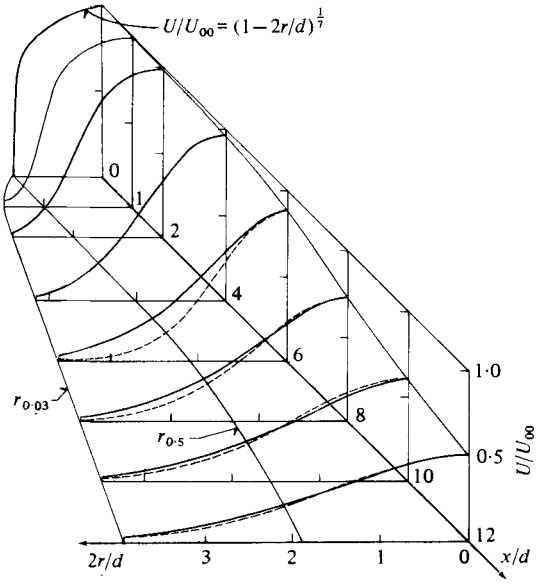


FIGURE 2. Radial distributions of the longitudinal mean velocity. ——, measurements ($U_{00}$ = 20 to 40 m/s); – – –, equation (1).

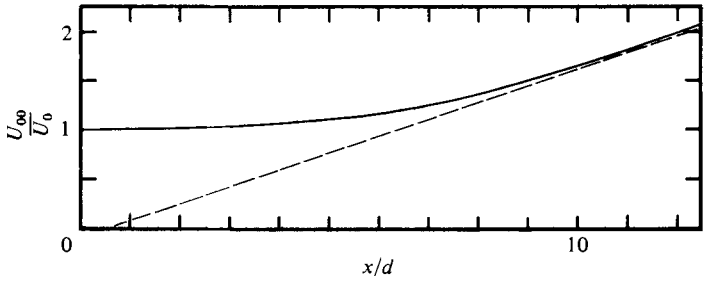


FIGURE 3. Centre-line velocity decay. ——, measurements; – – –, equation (2).

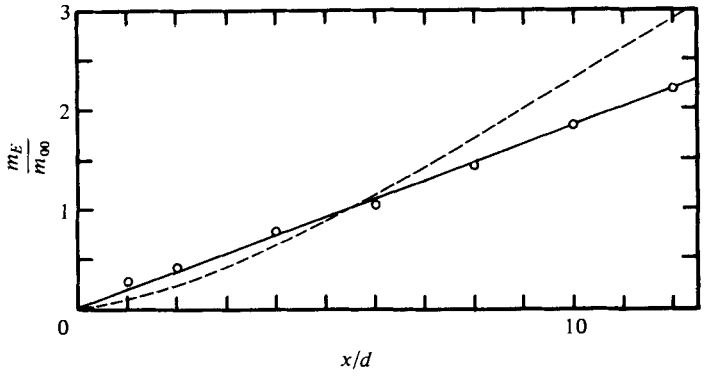


FIGURE 4. Entrainment rate distribution, where

$$m_{00} = 2\pi \int_0^{\frac{1}{2}d} \rho U r\, dr \quad \text{at} \quad x = 0, \quad m_x = 2\pi \int_0^{\infty} \rho U r\, dr$$

and $m_E = m_x - m_{00}$. ○, present results; – – –, Hill (1972); ——, $m_E/m_{00} = 0{\cdot}183\, x/d$.

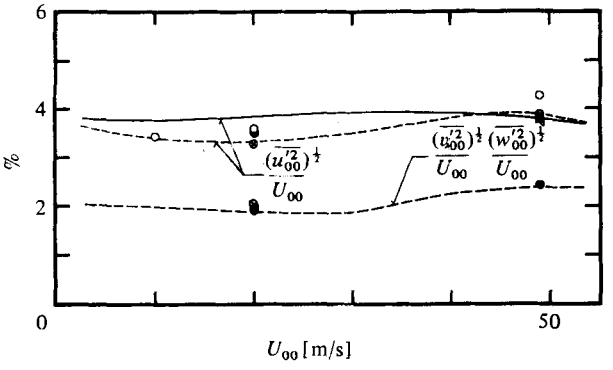


FIGURE 5. Turbulent intensities on the centre-line of the pipe. ○, single sensor; ⊗, X-sensor. $d$ = 38·5 mm, $L/d$ = 50, $t_{00}$ = 19 to 23 °C.

within $1 \leqslant x/d \lesssim 12$. This means that in the initial region of the jet the local entrainment coefficient $C = dm_{00}^{-1}(dm/dx) = 0{\cdot}183$ is constant, contrary to the result obtained by Hill (1972), who used a direct measurement method and a short nozzle.

The turbulence intensities were measured with an X-sensor and only the root mean square of the longitudinal fluctuations was obtained with a single sensor. Some idea of the spread of these measurements can be observed in figure 5, where the neglected effect of velocity on the turbulence intensities in the middle of the outlet section of the pipe is shown. The points represent the results obtained during different radial traverses. The variations of the relative mean longitudinal velocity and turbulent intensities along the jet centre-line are shown in figure 6. The relative transverse turbulent intensity distributions have almost the same shape as the longitudinal ones. This means that on the axis the longitudinal turbulence intensity is proportional to the transverse turbulence intensity. Within a distance of $4d$ to $9d$ from the nozzle one can observe a rapid increase in the turbulence intensity due to the extension of the mixing subregion over the whole cross-section of the jet. Beyond a distance of $9d$ the turbulence intensity still grows slowly. The results presented are consistent with those

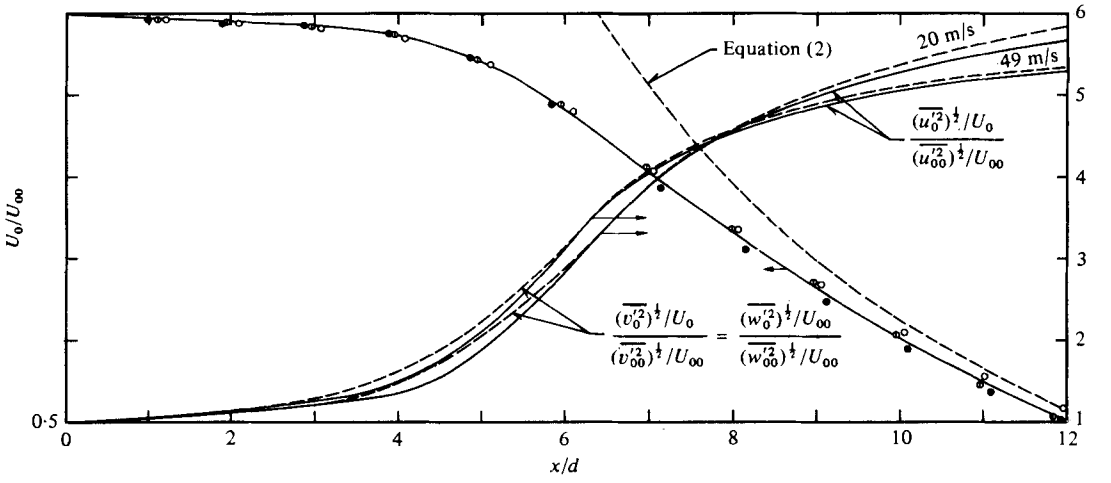


FIGURE 6. Axial variation of the longitudinal mean velocity and relative turbulent intensities on the jet centre-line. ○, $U_{00} = 20$ m/s; ⊙, $U_{00} = 30$ m/s; ●, $U_{00} = 49$ m/s. $(\overline{u'^2})^{\frac{1}{2}}/U_{00} = 3{\cdot}8 \pm 0{\cdot}1$ %, $(\overline{v'^2})^{\frac{1}{2}}/U_{00} = (\overline{w'^2})^{\frac{1}{2}}/U_{00} = 2{\cdot}2 \pm 0{\cdot}2$ %.

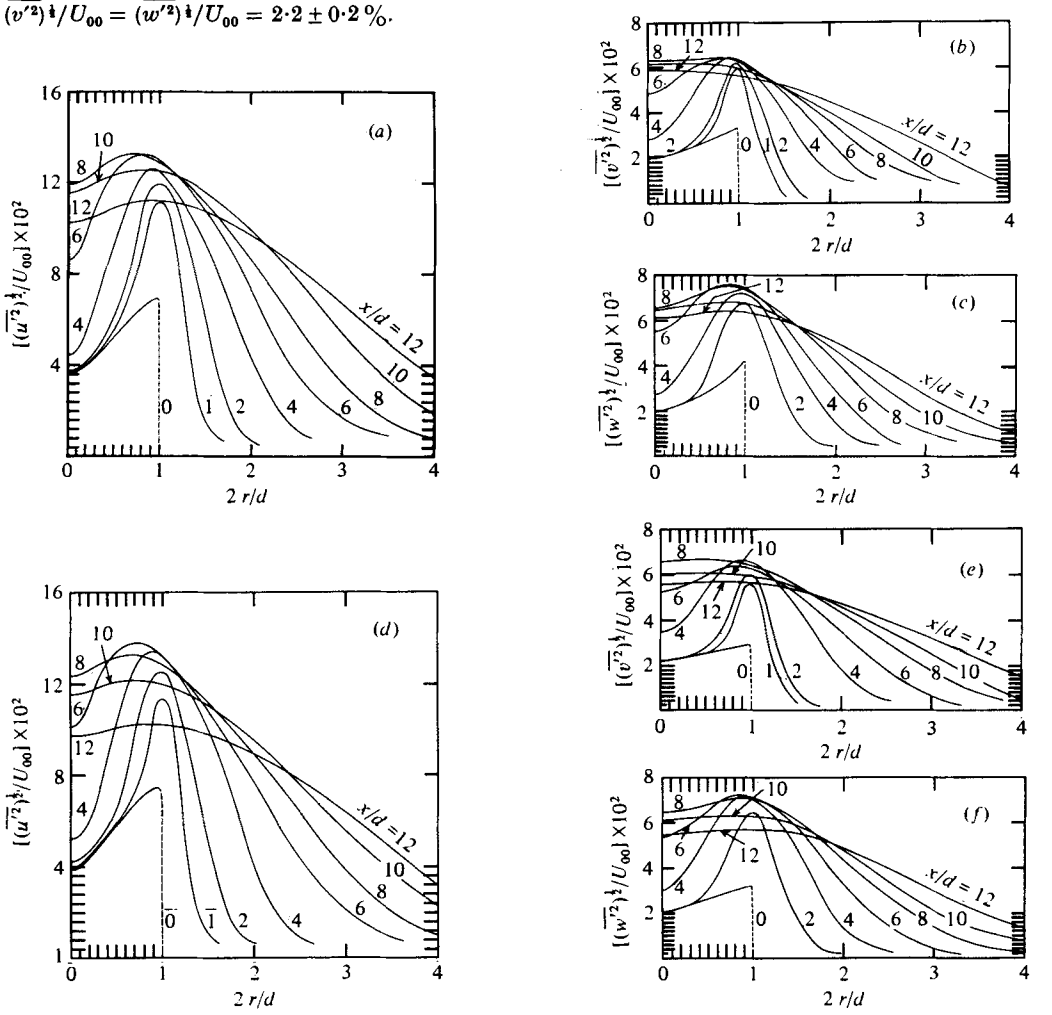


FIGURE 7. Evolution of the longitudinal $(\overline{u'^2})^{\frac{1}{2}}$, radial $(\overline{v'^2})^{\frac{1}{2}}$ and tangential $(\overline{w'^2})^{\frac{1}{2}}$ turbulence intensity profiles. (*a*)–(*c*) $U_{00} = 20$ m/s. (*d*)–(*e*) $U_{00} = 49$ m/s.

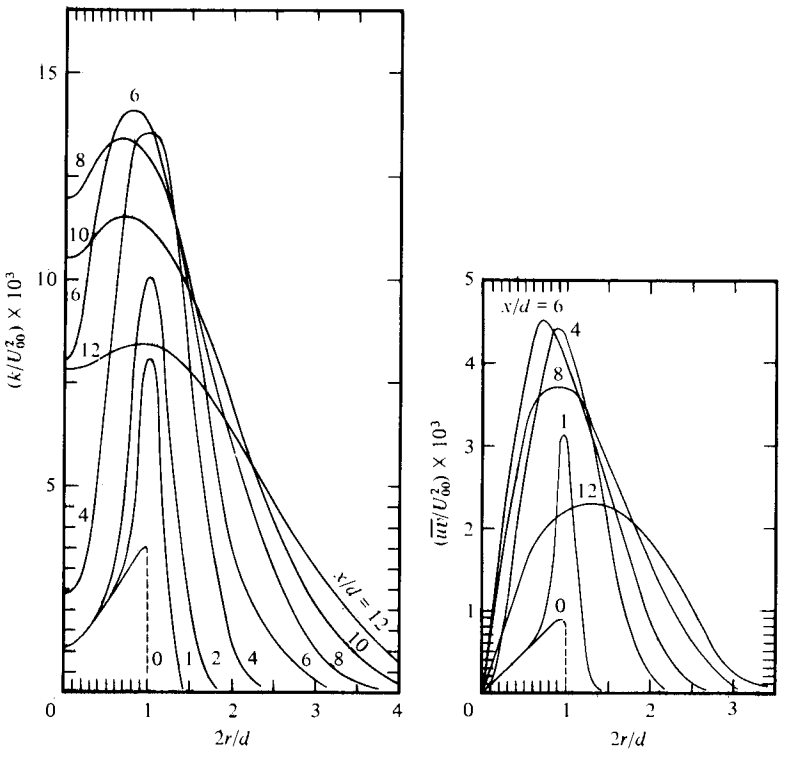


FIGURE 8. Turbulent kinetic energy and radial shear-stress distributions. $U_{00} = 49$ m/s.

obtained by Wygnanski & Fiedler (1969), where this growth takes place up to $40d$ for longitudinal values and up to $70d$ for the transverse ones.

The evolution of the longitudinal and transverse turbulence intensity profiles for efflux velocities of 20 and 49 m/s is shown in figure 7. The turbulence intensity first builds up at locations where the velocity gradient is high (in the mixing subregion) and further downstream turbulence of high intensity fills the whole cross-section of the jet. The profiles of the transverse intensities (radial and tangential) are very similar in shape and about half the size of the longitudinal ones.

The plot of turbulent kinetic energy against radius (figure 8*a*) has a very similar form to the previous plots. The highest peak of the turbulent energy occurs at an axial distance of $6d$ and radius $2r = (0{\cdot}7 \text{ to } 0{\cdot}8)d$, which is also the position of the highest peak of the shear-stress distributions (figure 8*b*). The depression at the axis occurs because there is still weak turbulence generation there. Thus the turbulent energy has to diffuse from the subregion where the turbulence is produced more intensively and, starting from a distance of $(8 \text{ to } 9)d$, is also transported (by convection and diffusion) from the regions of higher energy in the axial direction (see figure 9). In figure 9 one can discern a slight effect of the Reynolds number on the axial turbulent kinetic energy distribution. The maxima of the turbulent energy occur at distances of $7{\cdot}5d$ and $8{\cdot}5d$ for $Re = 51\,000$ and $125\,000$ respectively. However, in the developed region of the round jet the profile of turbulent kinetic energy does not show a minimum (figure 10) because the production of turbulent energy is relatively large at the centre-line (Rodi & Spalding 1970). It is interesting to notice that for the plane jet also a

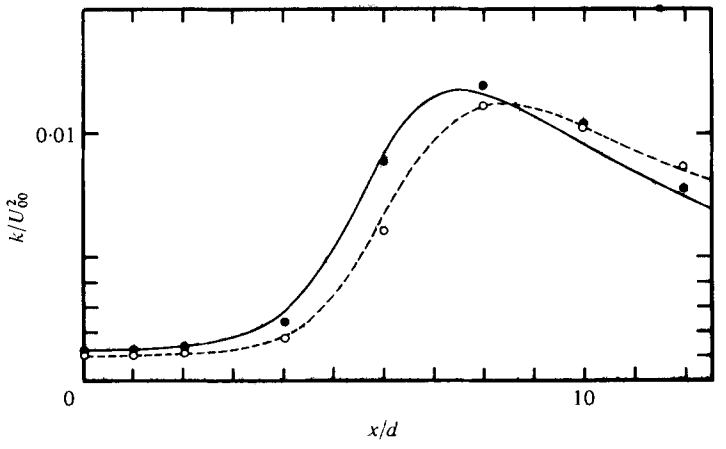


FIGURE 9. Centre-line turbulent kinetic energy distributions: $k = \frac{1}{2}(\overline{u'^2}+\overline{v'^2}+\overline{w'^2})$. ○, – – –, $U_{00} = 20\,\mathrm{m/s}$, $Re_{00} = U_{00}d/\nu = 51000$; ●, ——, $U_{00} = 49\,\mathrm{m/s}$, $Re_{00} = 125000$.

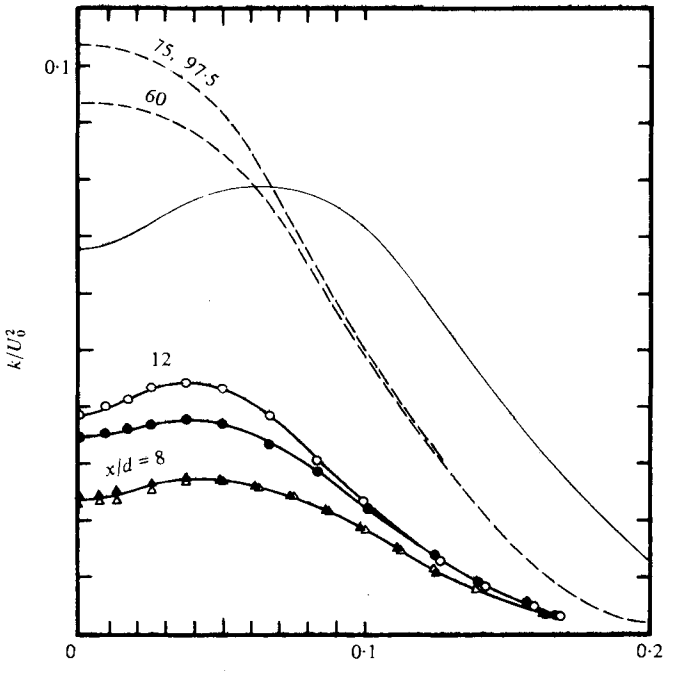


FIGURE 10 (*a*). For legend see next page.

trough occurs along the axis in the developed region. The turbulent energy in the developed region of the round jet is about 30 % higher than the value for the plane jet because strong longitudinal fluctuations can reach the axis from all radial directions (from the region of non-zero velocity gradient) and because of a more persistent character of turbulence with possibly toroidal vortices. All the results are consistent with those obtained by Wygnanski & Fiedler (1969) and Rodi (1975). Moreover the turbulent shear-stress distributions are consistent with the data of Donaldson *et al.* (1971) but the results of Sami *et al.* (1967) at a distance of 10*d* are twice as high as

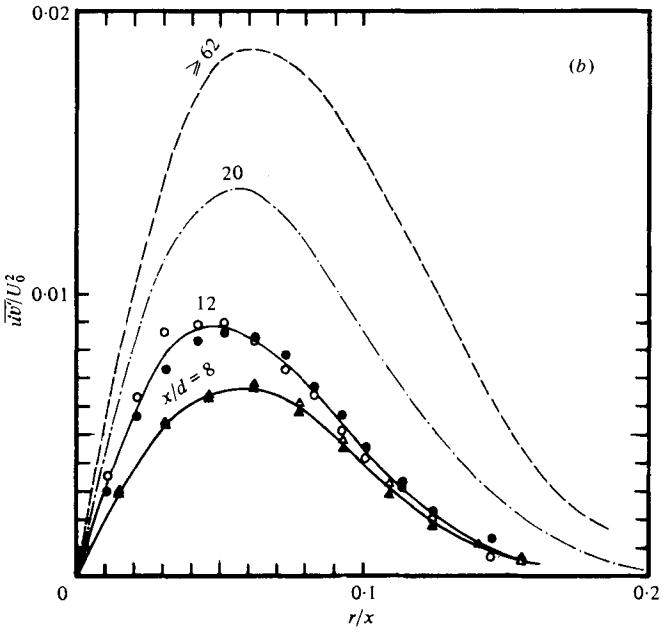


FIGURE 10. Normalized radial distributions of (*a*) the turbulent kinetic energy and (*b*) the shear stress. (*a*) – – –, Wygnanski & Fiedler (1969); ——, present results; ——, plane jet, Bradbury (1965). (*b*) —·—·—, Donaldson *et al.* (1971); △, $x/d = 8$, $U_{00} = 20$ m/s; ○, $x/d = 12$, $U_{00} = 20$ m/s; ▲, $x/d = 8$, $U_{00} = 49$ m/s; ●, $x/d = 12$, $U_{00} = 49$ m/s.

was expected. The radial profiles of the turbulent kinetic energy and shear stress reach a self-preserving form beyond a distance of about $75d$ and $60d$ respectively. However, in the initial region the normalized turbulent values tend towards their maximum values in the developed region whereas the absolute turbulent values have their ring-shaped maxima at a distance of about $6d$ and radius $2r = (0{\cdot}7 \text{ to } 0{\cdot}8)d$.

## REFERENCES

ABRAMOVICH, G. N. 1963 *The Theory of Turbulent Jets*. M.I.T. Press.

ABRAMOVICH, G. N., KRASHENINNIKOV, S. J., SEKUNDOV, A. N. & SMIRNOVA, I. P. 1974 *Turbulent Mixing of the Gas Jets* (in Russian). Moscow: Nauka.

BRADBURY, L. J. S. 1965 The structure of a self-preserving turbulent plane jet. *J. Fluid Mech.* **23**, 31.

CROW, S. C. & CHAMPAGNE, F. H. 1971 Orderly structure in jet turbulence. *J. Fluid Mech.* **48**, 547–591.

DONALDSON, C. DUP., SNEDEKER, R. S. & MARGOLIS, D. P. 1971 A study of free jet impingement. Part 2. Free jet turbulent structure and impingement heat transfer. *J. Fluid Mech.* **45**, 477–512.

GINIEVSKI, A. S. 1969 *Theory of Turbulent Jets and Wakes* (in Russian). Moscow: Mashinostroieniye.

HILL, B. J. 1972 Measurement of local entrainment rate in the initial region of axisymmetric turbulent air jets. *J. Fluid Mech.* **51**, 773–779.

HINZE, J. O. 1975 *Turbulence*. McGraw-Hill.

HINZE, J. O. & VAN DER HEGGE ZIJNEN, B. G. 1949 Transfer of heat and matter in the turbulent mixing zone of an axially symmetrical jet. *Appl. Sci. Res.* A **1**, 435–461.

LAU, C. J. & FISHER, M. J. 1975 The vortex-street structure of 'turbulent' jets. Part 1. *J. Fluid Mech.* **67**, 299–337.

POPIEL, CZ. O., KAMASA, A. & BOGUSŁAWSKI, L. 1976 Traversing mechanism. *Heat Transfer Section Ann. Rep., Tech. Univ. Poznań.*

RAJARATNAM, N. 1976 *Turbulent Jets.* Elsevier.

RODI, W. 1975 A new method of analysing hot-wire signals in highly turbulent flow, and its evaluation in a round jet. *DISA Inf.* **17**, 9–18.

RODI, W. & SPALDING, D. B. 1970 A two-parameter model of turbulence and its application to free jets. *Wärme Stoffübertragung* **3**, 85–95.

SAMI, S., CARMODY, TH. & ROUSE, H. 1967 Jet diffusion in the region of flow establishment. *J. Fluid Mech.* **27**, 231–252.

WYGNANSKI, I. & FIEDLER, M. 1969 Some measurements in the self-preserving jet. *J. Fluid Mech.* **38**, 577–612.